Applied Surface Science 37 (1989) 369–380
North-Holland, Amsterdam

TOPOLOGICAL STUDY OF THE MULTI-ALKALI PHOTOCATHODE DESTABILIZATION DUE TO MOLECULAR OXYGEN

J. PANCÍŘ and I. HASLINGEROVÁ

J. Heyrovský Institute of Physical Chemistry and Electrochemistry, Czechoslovak Academy of Sciences, Dolejškova 3, 182 23 Prague, 8, Czechoslovakia

Received 1 March 1989; accepted for publication 5 May 1989

A multi-alkali antimonide destabilization brought about by an interaction with such a common agent as molecular oxygen is studied theoretically. Adsorption energies and molecular diagrams of all phases which can temporarily exist in the Sb(NaKCs) multi-alkali photocathode systems were studied by the recently developed quantum chemical topological method. Systems under study were modelled as semi-infinite $(SbXYZ)_n$ crystals, X, Y, and Z being Na, K, or Cs. Calculations were performed with cubic and hexagonal crystal lattices. Molecular oxygen can substantially reduce the stability of photocathodes in which Sb and Cs atoms are present on their surface. The presence of even small amounts of oxygen in the surrounding medium should be avoided and/or surface Sb atoms should be adequately protected from the oxygen attack during the manufacturing of such photocathodes.

1. Introduction

The subject of this study is a theoretical investigation of alkali antimonide destabilization due to such a common impurity as molecular oxygen. The systems under study from commonly used multi-alkali photocathodes which exhibit the highest integral sensitivity of all photocathodes with a positive electron affinity which are produced nowadays. Alkali antimonides have been used commercially as photoemissive photon detectors for many years [1,2]. Among other properties, the stability of Sb(Na, K, Cs) systems is very important for their commercial utilization.

Surface layers were modeled by the semi-infinite $(SbXYZ)_n$ crystals, X, Y, and Z being Na, K, or Cs. Calculations were performed on cubic and hexagonal crystal lattices. The calculations were performed by a quantum-chemical topological method which has been developed recently by one of us [3].

2. Theoretical method and model systems

In the present study the same procedure has been used as in refs. [3–5] and we refer to these papers for details.

Table 1
Values of Coulomb integrals α in MJ/mol which were used in this study

Atom	α_s	α_p	α_d
Sb	−1.245	−0.669	0.0
Na	−0.402	−0.199	–
K	−0.287	−0.160	–
Cs	−0.272	−0.098	–
O	−0.635	−0.564	–

The parametrization procedure was the same as in paper [5]. Resonance integrals were calibrated on heats of formation of small molecules of similar valence types. In addition, orbital electronegativities (table 1), used as a basis for calculations of Coulomb integrals, were empirically scaled to reproduce correctly charge distributions in small systems [3]. The AO basis set consisted of 372 orbitals.

Similarly as in ref. [5] we used two model structures – cubic and hexagonal lattices. Models of these lattices are presented in figs. 1 and 2 in which elementary cells are outlined. The basic clusters to be calculated consisted of 6 crystallographic planes. Odd planes of the cubic lattice included 6 Sb atoms and 12 alkali atoms whereas even planes only 6 alkali atoms. Odd planes of

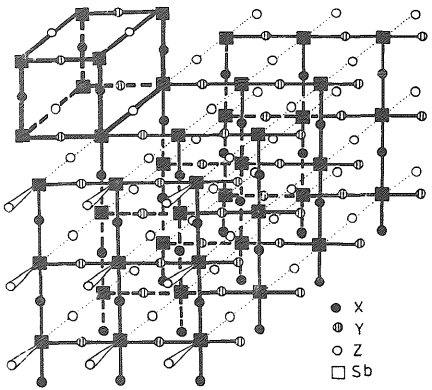

Fig. 1. Elementary cell and basic cluster of the cubic lattice. Atoms in planes parallel to the surface are linked by solid lines, atoms in successive planes are linked by dotted lines.

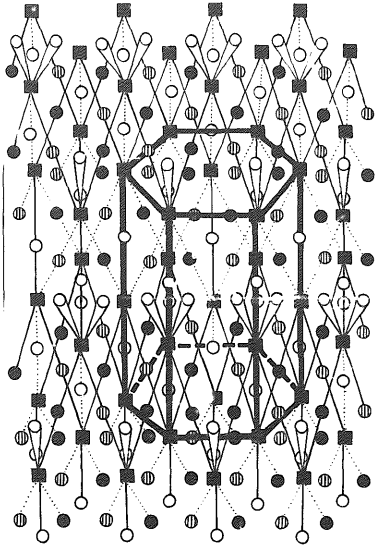

Fig. 2. Elementary cell and basic cluster of the hexagonal lattice. For further details see fig. 1.

the hexagonal lattice consisted of 6 Sb atoms and 9 alkali atoms whereas 3 other alkali atoms were lying on even planes. The proper symmetry of the infinite crystal in x- and y-dimensions was preserved by introducing periodic boundary conditions [5]. In addition, the uppermost of lowermost planes were fully saturated by molecular oxygen which was linked either to Sb atoms (the uppermost plane) or to alkali metals (the lowermost plane).

3. Results and discussions

In our calculations all possible combinations which can be formally derived by the replacement of Na, K, or Cs for X, Y, or Z in both lattice types $(SbXYZ)_n$ were considered. In this particular case the calculations were

Table 2
Adsorption energies of systems under study (kJ/mol)

Systems	Capture on Sb atoms		Capture on alkali atoms the third atom points to O_2	
	Hexagonal structure	Cubic structure	Hexagonal structure	Cubic structure
NaNaNa	−460	−441	30	28
NaNak	−515	−453	14	121
NaNaCs	−445	−418	−11	112
KKK	−577	−539	71	103
KKNa	−518	−513	67	58
KKCs	−607	−551	38	92
CsCsCs	−643	−613	55	30
CsCsK	−612	−598	68	54
CsCsNa	−553	−569	30	−60
CsNaK	−673	−52	39	111

performed for 10 structures in both hexagonal and cubic lattices, each for both surface types of O_2 coverages.

Adsorption energies and molecular diagrams of all these systems are presented in table 2 and in figs. 3 and 4. In these figures only one "chain of

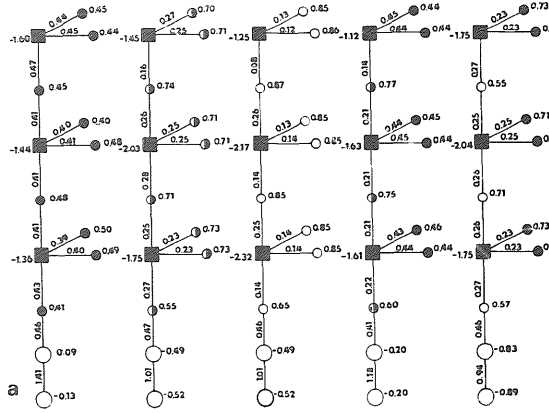

Fig. 3a. Molecular diagrams of cubic lattices of Na_3Sb, K_3Sb, Cs_3Sb, Na_2KSb, and Na_2CsSb systems with molecular oxygen absorbed on the alkali metal sides. Squares, closed circle, half-filled circle, small open circle, large open circle stand for Sb, Na, K, Cs, and O, respectively.

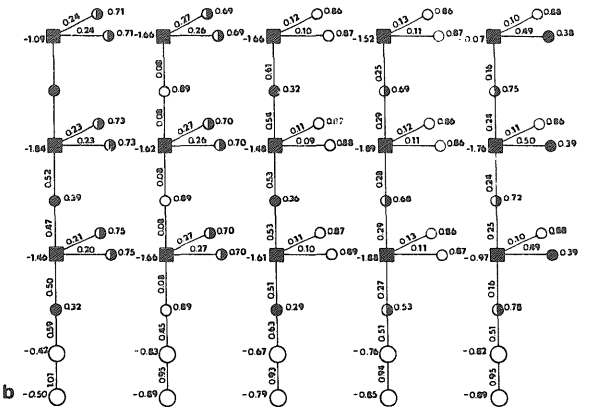

Fig. 3b. Molecular diagrams of cubic lattices of K_2NaSb, K_2CsSb, Cs_2NaSb, Cs_2KSb, and CsNaKSb systems. For further explanation see fig. 3a.

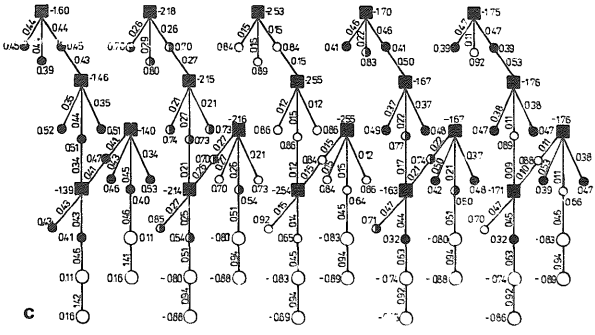

Fig. 3c. Molecular diagrams of hexagonal lattices on Na_3Sb, K_3Sb, Cs_3Sb, Na_2KSb, and Na_2CsSb systems. For further explanation see fig. 3a.

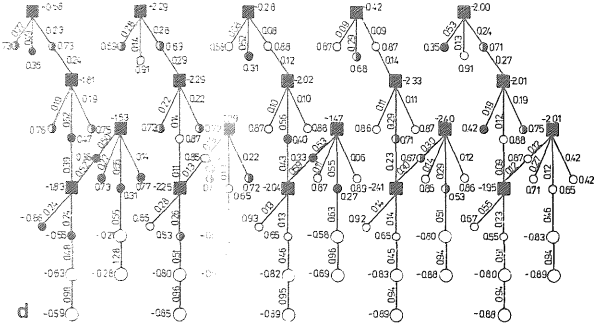

Fig. 3d. Molecular diagrams of hexagonal lattices of K_2NaSb, K_2CsSb, C_2NaSb, Cs_2KSb, and CsNaKSb systems. For further explanation see fig. 3a.

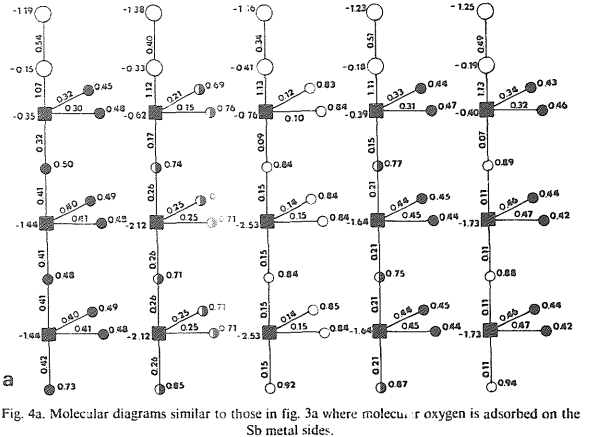

Fig. 4a. Molecular diagrams similar to those in fig. 3a where molecular oxygen is adsorbed on the Sb metal sides.

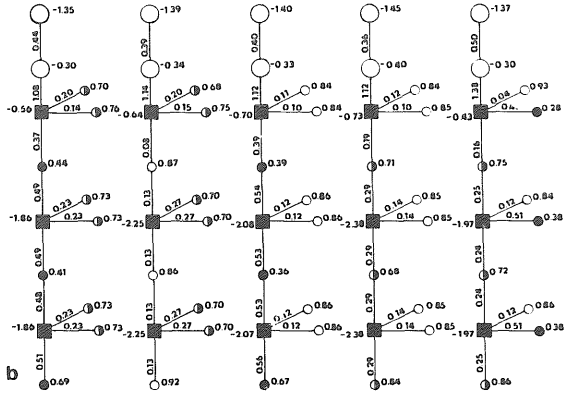

Fig. 4b. Molecular diagrams similar to those in fig. 3b where molecular oxygen is adsorbed on the Sb metal sides.

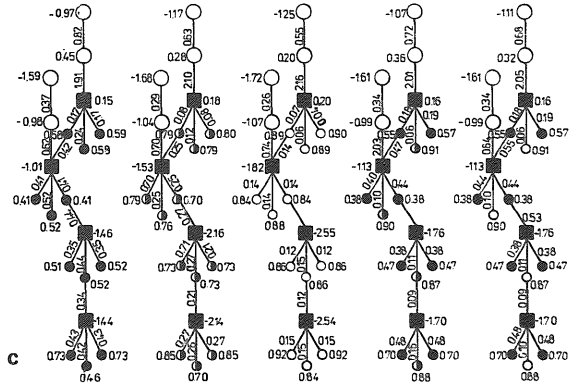

Fig. 4c. Molecular diagrams similar to those in fig. 3c where molecular oxygen is adsorbed on the Sb metal sides.

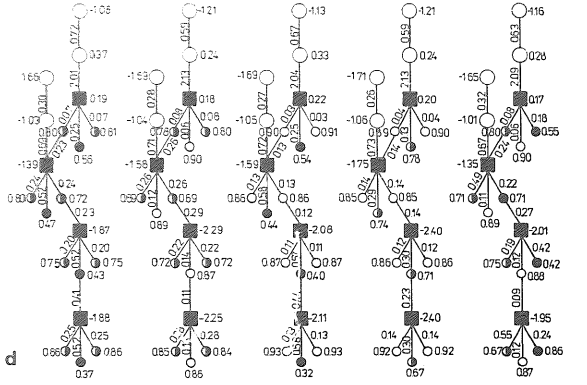

Fig. 4d. Molecular diagrams similar to those in fig. 3d where molecular oxygen is adsorbed on the Sb metal sides.

atoms" is presented which points from the uppermost plane to the lowermost plane. These elementary structural units repeat in directions of x- and y-axes through the system.

Specific adsorption energies ΔE are given in table 2. (The more negative the value of ΔE the more feasible it is for an attack to occur.) Because of the semi-empirical approximations used these values are not exact. However, we have assured ourselves in other fields of surface chemistry [4,6–11] that in a set of structurally similar lattices these values correspond to relative stabilities which are in good accord with the experiments. In this case, the binding of O_2 is somewhat stronger in hexagonal lattices than in cubic lattices, the attack of Sb being extremely feasible. This attack will be hindered by the increase of the concentration of Na atoms. The reason for the activity of Sb can be seen in the molecular diagrams of figs. 3 and 4. It can be seen that the O_2 attack on alkali atoms resembles a formation of alkali superoxides with a very weak alkali–O bond as is seen from corresponding bond orders. However, the attack on Sb results in the oxide-like formation with a strong Sb–O bond. This effect, together with the existence of free valence electrons in surface Sb atoms, is probably the explanation for this behavior. Moreover, the strong charge flux from Sb to the terminal oxygen gives rise to the strongly reactive Sb–O–O^- species with the possibility to release O^- ions.

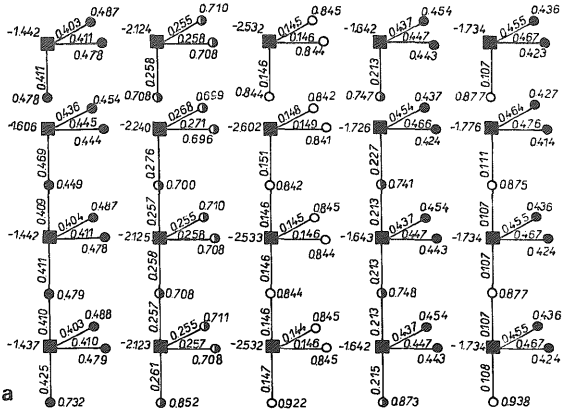

Fig. 5a. Molecular diagrams similar to those in fig. 3a which represent the parent systems. This figure is taken from ref. [5].

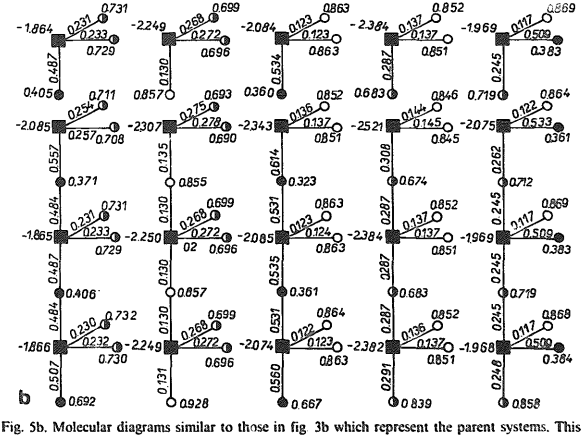

Fig. 5b. Molecular diagrams similar to those in fig. 3b which represent the parent systems. This figure is taken from ref. [5].

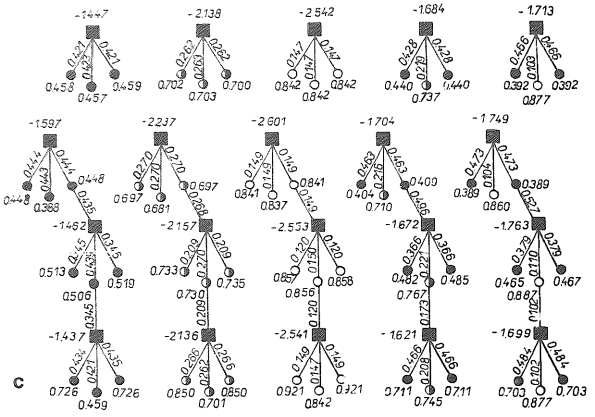

Fig. 5c. Molecular diagrams similar to those in fig. 3c which represent the parent systems. This figure is taken from ref. [5].

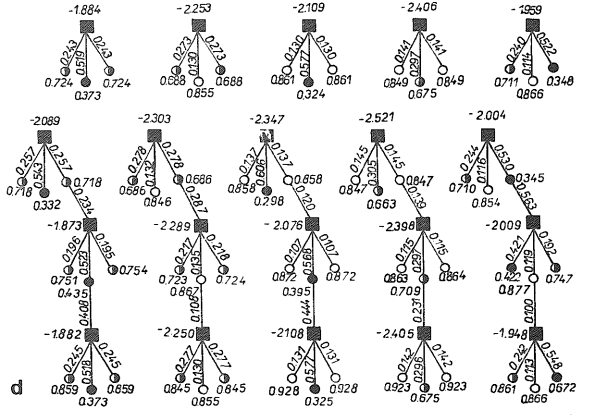

Fig. 5d. Molecular diagrams similar to those in fig. 3d which represent the parent systems. This figure is taken from ref. [5].

Table 3
Energies of HOMO's and LUMO's (kJ/mol)

Systems	Capture on Sb atoms				Capture on alkali atoms the third atom point to O_2			
	Hexagonal structure		Cubic structure		Hexagonal structure		Cubic structure	
	E_H	E_L	E_H	E_L	E_H	E_L	E_H	E_L
NaNaNa	−648	−588	−762	−760	−710	−709	−794	−794
KKK	−635	−543	−750	−750	−690	−685	−792	−792
CsCsCs	−628	−616	−743	−742	−670	−665	−786	−786
NaNaK	−644	−583	−761	−759	−705	−687	−793	−793
NaNaCs	−641	−580	−761	−759	−703	−670	−793	−790
KKNa	−639	−554	−751	−750	−704	−703	−792	−792
CsCsNa	−632	−552	−744	−744	−689	−688	−788	−787
KKCs	−633	−538	−750	−749	−689	−668	−789	−788
CsCsK	−630	−522	−743	−743	−681	−678	−787	−787
CsNaK	−636	−502	−756	−754	−697	−669	−792	−790

To compare the bond strengths after the oxygen attach we can compare corresponding bond orders of these structures with those of parent systems (fig. 5) which are taken from ref. [5]. In this figure the upper diagrams corresponds to the reference structures of systems which are infinite in all three dimensions. It is seen that the attack of alkali atoms brings no significant changes in the whole structure. However, substantial reduction of bond orders and thus bond strengths can be found in the surface layer of alkali–Sb bonds. The particularly strong bond strength reduction appears with Sb–Cs bonds. It can thus be concluded that the absorption of O_2 on Sb atoms can lead to the release of surface Cs atoms and to the breakdown of the crystal surface.

Energies of highest occupied molecular orbitals (HOMO's) and lowest unoccupied molecular orbitals (LUMO's) are presented in table 3. Similarly as with bonding energies these values should be regarded as relative. By inspection of table 3 can be seen that the arithmetic mean of HOMO's and LUMO's, which can be related to the electronic work function bears lower values with the increasing concentration of Cs atoms. However, by comparing tables 2 and 3, it should be clear that the decrease of the work function is associated with the decrease of the stability.

4. Conclusion

It can be concluded that the presence of the molecular oxygen can considerably affect the stability of the multi-alkali photocathodes, particularly, if Sb atoms are present on the surface. Possible damage is the release of free Cs

atoms which is followed by surface reconstruction. The possible preservation is to make the preparation in a strongly reductive environment and/or to prevent the existence of Sb particles on the surface. Finally, we should remark that the stability of multi-alkali photocathodes towards other possible contaminating agents such as nitrogen and carbon-containing species is a topic which will be further studied in this laboratory.

Acknowledgement

This paper required a rather high level of skill in figure-drawing. The authors are greatly indebted to Miss Dita Jonášová for her valuable technical help.

References

[1] A.H. Sommer, Photoemissive Materials (Wiley, New York, 1981).
[2] L. Galan and C.W. Bates, J. Phys. D (Appl. Phys.) 14 (1981) 293.
[3] J. Pancíř, Collection Czech. Chem. Commun. 45 (1980) 2452, 2463.
[4] J. Pancíř, I. Haslingerová and P. Nachtigall, Surface Sci. 181 (1987) 413.
[5] J. Pancíř, I. Haslingerová and P. Nachtigall, Appl. Surface Sci. 25 (1986) 167.
[6] J. Pancíř, I. Haslingerová and P. Nachtigall, Chem. Phys. 119 (1988) 289.
[7] J. Pancíř, J. Horák and Z. Starý, Phys. Status Solidi (a) 103 (1987) 517.
[8] J. Pancíř, I. Haslingerová and P. Nachtigall, Collection Czech. Chem. Commun. 53 (1988) 2064.
[9] J. Pancíř and I. Haslingerová, Collection Czech. Chem. Commun., in press.
[10] J. Pancíř and I. Haslingerová, Czech. J. Phys., in press.
[11] J. Pancíř and I. Haslingerová, Appl. Surface Sci., to be published..